

# Aspect ratio-dependent optical properties of Ni–P/AAO nano-array composite structure

Feng-Hua Wang · Ya-Fang Tu · Jian-Ping Sang ·  
Sheng-You Huang · Xian-Wu Zou

Received: 19 August 2009 / Accepted: 17 March 2010 / Published online: 30 March 2010  
© Springer Science+Business Media, LLC 2010

**Abstract** Using electrochemical deposition, Ni–P nanorod arrays with a series of aspect ratios have been successfully fabricated in the pores of anodic aluminum oxide (AAO) membranes. The aspect ratio of Ni–P nanorods was controlled by the deposition time. The morphologies were analyzed by scanning electron microscopy and transmission electron microscopy. The dependence of the optical absorbance upon the aspect ratio was studied by UV–vis spectra. The results show that the absorbance increases in visible region and decreases rapidly in ultraviolet region as the aspect ratio of nanorods increases, which qualitatively agree with the prediction of Maxwell–Garnett (MG) theory and the simulation based on the Mie scattering theory, respectively. The dependence of photoluminescence emission (PL) spectra upon the aspect ratio is also obtained. These investigations show that the optical properties of nano-array composite structure can be modified by changing the aspect ratio of nanorods.

## Introduction

High aspect ratio nanostructures such as nanorods, nanotubes, and nanowires have attracted considerable attention [1–5] due to their novel properties and potential applications in electronics, magnetics, photonics, optoelectronics, and biological sensors. Among varied composite nanostructures,

the nanorod/AAO composite structures are noticeable. Based on the anodic aluminum oxide (AAO) membranes, various composite nanostructures containing metallic [6–8] and semiconductive [9, 10] nano-arrays have been fabricated. By adjusting the fabrication conditions, the nanorod/AAO composite structures consisting of AAO membrane and aligned nanorods with well-defined diameter, aspect ratio, and orientation were obtained. Furthermore, since the AAO membrane is transparent over large segments of the visible and infrared spectral regions, the characterization of the optical properties of the nanorod/AAO composite structure has also been quite straightforward [11–15].

Ni–P/AAO nano-array composite structure is one of the alloy/AAO nanostructures. As block materials, amorphous Ni–P alloys [16] have been extensively used for different applications, because of their excellent mechanical, physical, electrical, corrosion, and wear-resistance properties. To construct composite nanostructures, Chiriac et al. [17] fabricated amorphous Ni–P nanowire arrays by electrodepositing Ni–P nanowires with diameters of 200 nm into the nanopores of the AAO membrane and investigated the effect of composition on the magnetic properties. However, there is still reduced information concerning the investigation of the optical properties of Ni–P/AAO nano-array composite structures. It was found that the physical properties of nanorod/AAO composite structure depend not only upon the properties of component materials but also upon the morphologies and structure of the composite structure assembly. Although the optical properties of metal particles were described by Mie's theory in 1908, the relationship between the particle geometry and their optical properties has not been fully established [18]. Recent years, investigations on the dependence of optical absorbance upon the nanorod aspect ratio were carried out for Au [19], Ag [20], and Ni [21] nanorod arrays embedded in

F.-H. Wang · J.-P. Sang (✉) · S.-Y. Huang · X.-W. Zou  
Department of Physics, Wuhan University,  
Wuhan 430072, China  
e-mail: jpsang@acc-lab.whu.edu.cn

Y.-F. Tu · J.-P. Sang  
Department of Physics, Jianghan University,  
Wuhan 430056, China

membranes. The obtained relationship between the nanorod aspect ratio and optical properties is qualitatively consistent with the predictions of Maxwell–Garnett (MG) theory. All of these investigations were made in the case that the radius of nanorods was much smaller than the wavelength of incident light ( $R \ll \lambda$ ) in which case M–G theory was suitable. However, it is unknown how the optical absorbance depends upon the nanorod aspect ratio and what theory is suitable when  $R$  is not negligibly small compared to the wavelength. In addition, previous investigations were concerned in pure metals, what will happen for Ni–P nanorod array? To answer the questions mentioned above, in this paper we studied the dependence of optical absorbance upon the Ni–P nanorod aspect ratio in two cases:  $R \ll \lambda$  and  $R$  is not negligibly small compared to the wavelength  $\lambda$ . For these two cases different behavior of absorption was revealed and suitable theory was designated.

## Experiment

The AAO membrane was prepared by anodizing a high-purity Al foil in an acid solution using a two-step process [22, 23]. The aluminum foils (99.95 %) were first degreased, annealed at 400 °C for 3 h, and then electropolished in a 1:4 volume mixture of perchloric acid and ethanol at 16 V for 3 min to a mirror finish. As the first step, the clean aluminum foils were anodized in a 0.3 mol/L oxalic acid solution at 40 V and at 17 °C for 10 h. A preliminary alumina layer was obtained. This alumina layer was removed by immersing the sample in a mixture of phosphoric acid (6 wt%) and chromic acid (1.8 wt%) aqueous solution at 60 °C for 3 h. Then the second step of anodization was carried out. The anodization time was determined by the required thickness of the AAO membrane [24]. For an applied voltage of 40 V and an anodization time of 1.5 h, the pore diameters were about 50 nm. In order to electrodeposit samples with low voltage, a thinning process for the barrier layer at the pore base should be added before electrodeposition. After the AAO membrane formed, the anodic voltage was decreased gradually from 40 to 7 V which lasted for 20 min and then kept at this voltage for 5 min. The electrolyte solution consisted of nickel sulfate 25 g L<sup>-1</sup>, sodium hypophosphite 25 g L<sup>-1</sup>, and sodium citrate 15 g L<sup>-1</sup>, and the pH was in the range of 4.7–4.9. The electrodeposition was carried out at room temperature and at 9 V ac (50 Hz) for several minutes using Pt plate as a counter electrode and AAO template with aluminum plate as a working electrode. After that, The AAO membranes containing ordered Ni–P nanorod array were then removed from the Al substrates using aqueous HgCl<sub>2</sub>. Consequently, the Ni–P/AAO nano-array composite

structures with different aspect ratios of nanorods were obtained.

A thin platinum layer was sputtered using a current of 30 mA for 80 s to form a conducting film of about 5–6 nm thickness for the use of observation. The microstructure and morphology were characterized by scanning electron microscopy (SEM, FEI SIRION Field Emission Gun) and transmission electron microscopy (TEM, JEOL JEM-2010). For SEM observation, the Ni–P/AAO composite structure was immersed in a mixture of phosphoric acid (6 wt%) and chromic acid (1.8 wt%) at 60 °C for 10 min. After this process, the alumina from the surface layer of the template was removed and the ordered Ni–P nanorod array revealed. The samples for TEM were treated by using 5 wt% NaOH solutions for 40 min to dissolve the AAO membrane, and then ultrasonically dispersed in ethanol. Optical absorption spectra were recorded at room temperature using a UV–VIS dual-beam spectrophotometer. The photoluminescence emission (PL) spectral measurements were carried out on the HITACHI F-4500 Fluorescence Spectrophotometer using the excitation wavelength of 350 nm.

## Results and discussion

The template syntheses method allows for straightforward control of nanorod size, shape, and orientation. We synthesized a set of Ni–P/AAO composite structures consisting of Ni–P nanorods with different length by electrodeposition. Figure 1 shows the top view SEM image of the electrodeposited Ni–P/AAO composite structure. This image displays a uniform and highly packed Ni–P nanorod array. It can be seen that the diameter of Ni–P nanorod is about 50 nm. The morphology and microstructure of the Ni–P nanorods are observed and they are presented in Fig. 2. Figure 2a, b shows the typical SEM images of cutaway

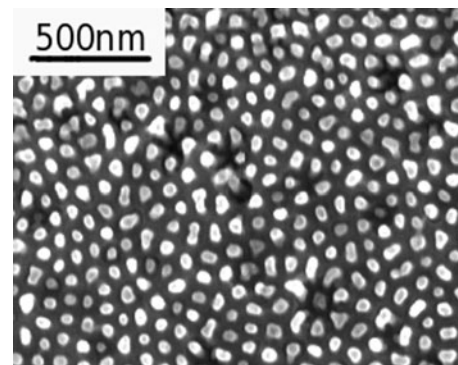


**Fig. 1** Top view SEM image of synthesized Ni–P/AAO nano-array composite structure. To make the Ni–P nanorod array clear, the alumina in the surface layer of the template was removed

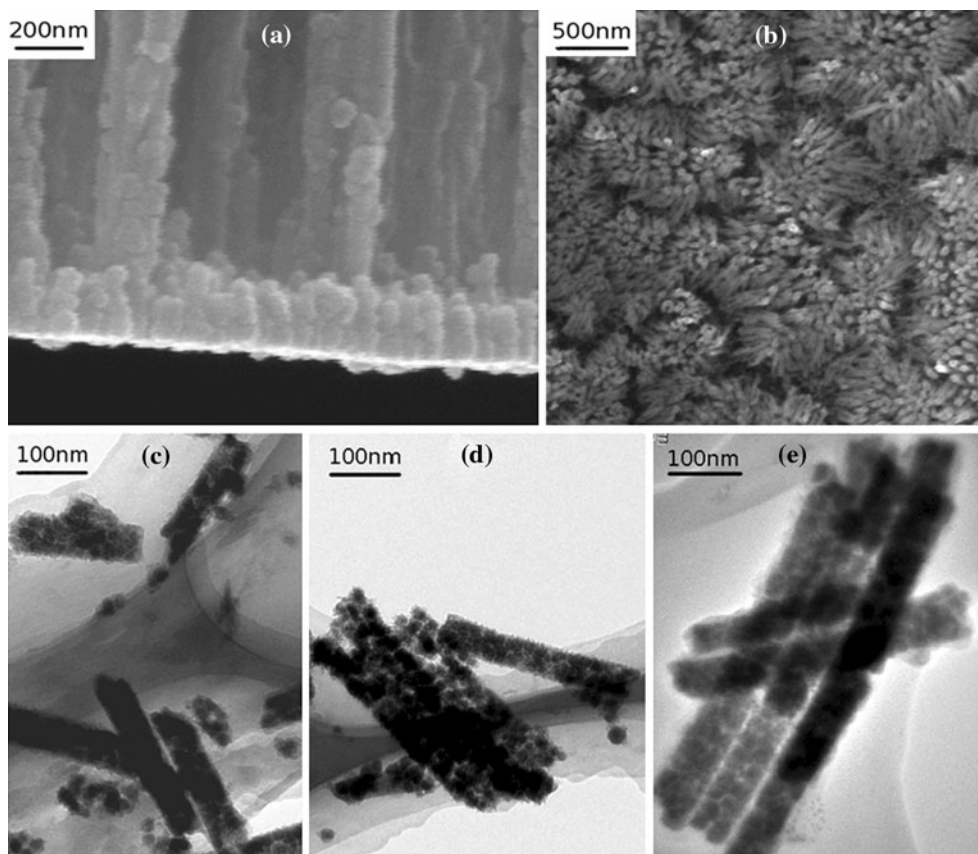


**Fig. 2** Micrographs of the Ni–P/AAO nano-arrays prepared by electrodeposition at 9 V ac for different deposition time. **a** The SEM image of cutaway view of the composite structure prepared by electrodeposition for 3 min. The alumina in the surface layer of the sample has been dissolved, so a part of Ni–P nanorods becomes

visible. **b** The SEM image of top view of the composite structure prepared by electrodeposition for 5 min. Since alumina in the surface layer of the sample has been removed, the Ni–P nanorods gather and form nanorod clusters. **c–e** Are the TEM images of the Ni–P nanorods prepared by electrodeposition for 3, 5, and 13 min, respectively

view and top view of the composite structure. These two samples were fabricated by electrodeposition for 3 and 5 min, respectively. Corresponding TEM images of the two samples are given in Fig. 2c, d. Figure 2c shows that for the sample fabricated by short time electrodeposition (3 min) the Ni–P nanorods are short with an average length of 215 nm, which is identical to the dimension of Ni–P nanorods in Fig. 2a. Figure 2d displays that for the sample prepared by intermediate time electrodeposition (5 min) the average length of Ni–P nanorods is 325 nm. A TEM image of the sample prepared by long time electrodeposition (13 min) is shown in Fig. 2e. In this case, the Ni–P nanorods become longer (590 nm), but the cylindrical radius hold constant by the pore walls of AAO membrane. Figure 3 summarizes the measured relationship between the aspect ratio of nanorod and deposition time, which is obtained from TEM images. It can be seen that during the initial stage of the deposition, the aspect ratio increases quickly with the increase of deposition time. When the deposition time reaches 13 min, the aspect ratio does not

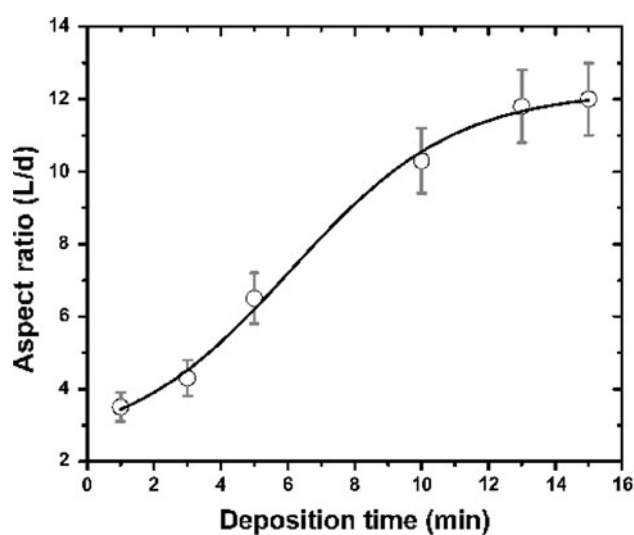


**Fig. 3** Dependence of the aspect ratio ( $L/d$ ) of the Ni–P nanorod on the electrodeposition time for Ni–P/AAO composite structure assemblies.  $L$  is the length and  $d$  is the diameter of the Ni–P

vary with deposition time any more. According to the ac electrodeposition mechanism, when the oxidation and deoxidization reaches a balance, the net electrodeposition weight of Ni–P does not increase any more. For the five samples, the nano aspect ratio,  $L/d$ , is 3.5, 4.3, 6.5, 10.3, 11.8, for deposition times of 1, 3, 5, 10, 13 min, respectively.

To investigate the variation of the optical absorbance spectra with the aspect ratio, we measured the optical absorption spectra and PL spectra for the Ni–P/AAO composite structures with a set of aspect ratios ( $L/d = 3.5, 4.3, 6.5, 10.3$ , and 11.8). The results are shown in Fig. 4. To make a comparison, corresponding optical spectra of the blank AAO membrane are shown in the same figure. The optical absorbance spectra of Ni–P/AAO composite structures are quite different from that of the blank AAO membrane. As the aspect ratios,  $L/d$ , ( $L/d \geq 4.3$  specially) increases, the optical absorbance of the Ni–P/AAO composite structure decreases rapidly in the ultraviolet region and increases in the visible region.

In the following we try to explain the variation of the optical absorbance spectra with the aspect ratio. There are opposite behaviors in the visible and ultraviolet regions. First we explain the behavior in the visible region. Up to now, many studies have reported the phenomenon that the nanorod/AAO composite structures with larger aspect ratio have larger absorbance in the visible and IR regions [12, 25–29]. Some authors attributed this characteristic to surface plasmon resonance [25, 26], polarization effect [27], or field enhancement factor [19]. The others derived this behavior by using the MG effective medium theory [12, 28] and finite-difference time-domain (FDTD) simulation [29]. By comparison, MG theory is valid when nanorod dimensions are much smaller than the wavelength of light [12]. The simulation spectra obtained using MG theory are qualitatively in agreement with the experimental results on the dependence of the optical absorption spectra upon the aspect ratio in the visible region [28].

According to the MG effective medium theory, as the radius of particles is much smaller than the incident

wavelength (e.g., radius  $R \leq 0.1 \lambda$ ), the total absorption coefficient  $\alpha$  can be given via the expression [30]

$$\alpha = \frac{18\pi f \varepsilon_0^{3/2} \varepsilon_2}{(\varepsilon_1 + \kappa \varepsilon_0)^2 + \varepsilon_2^2} \frac{1}{\lambda} = \frac{A}{\lambda},$$

$$A = \frac{18\pi f \varepsilon_0^{3/2} \varepsilon_2}{(\varepsilon_1 + \kappa \varepsilon_0)^2 + \varepsilon_2^2}, \quad (1)$$

where  $f$  is the volume-filling fraction of particles,  $\lambda$  is the incident wavelength.  $\varepsilon_1$  and  $\varepsilon_2$  are the imaginary part and real part of the complex dielectric function of the particles and  $\varepsilon_0$  is the dielectric constant of the surrounding environment. The screening factor,  $\kappa$ , is related to the depolarization factor  $q$  as [31]

$$\kappa = \frac{1-q}{q} \quad (2)$$

The depolarization factor depends on the geometry of the particles and its orientation with respect to the electric field. For simplicity, we assume that the Ni–P nanorods can be treated as ellipsoidal elongated particles. When the axis of the nanorod is parallel with the incidence vector and hence perpendicular to the electric field, the relation between the depolarization factor  $q$  and the size of the nanorod can be expressed as [32]

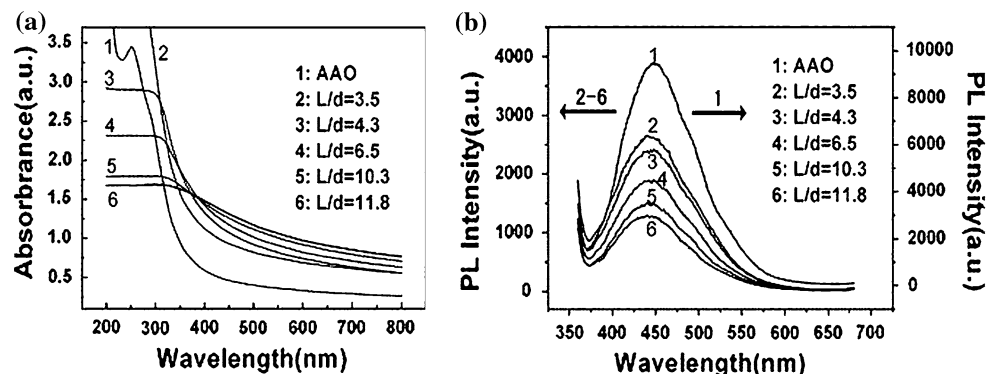
$$q \approx \frac{L}{d + 2L} \quad (3)$$

Substituting Eq. 3 into Eq. 2, we obtain

$$\kappa \approx 1 + \frac{d}{L} \quad (4)$$

According to Eq. 1,  $A$  can be expressed by  $f$ ,  $\varepsilon_1$ ,  $\varepsilon_2$ , and  $\kappa$ . For Ni–P/AAO composite structures deposited in the same conditions, the composition of Ni–P nanorods is certain so  $A$  is mainly determined by  $f$  and  $\kappa$ . On the other hand, for a certain nanorod diameter, the increasing of the aspect ratio,  $L/d$ , makes the volume-filling fraction of Ni–P nanorods  $f$  increasing,  $\kappa$  decreasing, and the absorption coefficient  $\alpha$  rising. Our experiment is also consistent with

**Fig. 4** Optical spectra of blank AAO membrane and Ni–P/AAO nano-array composite structures with a series of aspect ratios ( $L/d$ ). **a** UV–vis absorption spectra. **b** PL spectra recorded at room temperature with the laser excitation of 350 nm



the absorption behaviors of ordered-arrays Au nanowires ( $R = 10$  nm,  $\lambda = 400\text{--}1800$  nm,  $L/d = 23, 30, 43, 70$ ) [19]. Therefore, the optical absorbance of the Ni–P/AAO composite structure increases with the increasing of the nanorod aspect ratio in the visible region. It corresponds to the right part of Fig. 4a.

Next we explain why the optical absorbance of the Ni–P/AAO composite structure decreases with the increase of the nanorod aspect ratio in the ultraviolet region. It is well known that the MG theory is only suitable for nanorods with a much smaller radius than the wavelength of incident light [31]. In the present work, the diameter of the Ni–P nanorods is 50 nm and the dimension and mutual separation distance of Ni–P nanorods are much smaller than the wavelength of visible light, so scattering effects can be negligible in the visible region [33]. However, compared to the wavelength of ultraviolet light, the dimensions of Ni–P nanorods are not negligibly small and it is necessary to consider more rigorous scattering theories [34]. The scatter capability can be expressed by the scattering cross section. According to the Mie scattering theory [35] for ellipsoids of revolution or otherwise axisymmetric particles, the extinction cross section is given by [36, 37]

$$C_{\text{sca}} = \frac{\lambda^2}{2\pi} \sum_{\sigma=1}^2 \sum_{m=0}^{\infty} \sum_{n=m}^{\infty} D_{\sigma mn} \text{Re}\{f_{\sigma mn} + g_{\sigma mn}\}, \quad (5)$$

where  $f_{\sigma mn}$  and  $g_{\sigma mn}$  are the scattering coefficients for the magnetic and electric fields, respectively, and  $\sigma$ ,  $m$ , and  $n$  are the expansion indices of vector spherical harmonic functions.  $D_{\sigma mn}$  is a normalization constant. “Re” specifies the real part of  $(f_{\sigma mn} + g_{\sigma mn})$ . The calculation of  $f_{\sigma mn}$  and  $g_{\sigma mn}$  is not trivial and has been done for ellipsoids by the “separation-of-variables” method [38] and the so-called “T-matrix” method [39]. Al-Rawashdeh et al. [34] calculated the normalized extinction coefficient spectra of Au ellipsoids with the diameter of 120 nm for a series of aspect ratios in the wavelength range from 400 to 900 nm by using the T-matrix method. It can be seen from Fig. 12 of Ref. [34] that in the short wavelength region (400–600 nm), the calculated extinction coefficient spectrum shows that the extinction coefficient decreases as the aspect ratio increases. This result from the T-matrix scattering calculation is consistent with our measurements for Ni–P/AAO composite structures, in which the absorbance decreases with the increment of aspect ratio in the wavelength range from 200 to 350 nm (see Fig. 4a).

We measured the PL spectra for the blank AAO membrane and Ni–P/AAO composite structures with a series of aspect ratios. The results are shown in Fig. 4b. It can be seen that in the PL spectrum, a peak appears at about 450 nm and the peak intensity decreases with the increase of the nanorod aspect ratio  $L/d$ . On the other hand, in

Fig. 4a Ni–P/AAO nano-array composite structure has a strong absorbance as  $\lambda > 350$  nm, and the larger the aspect ratio is, the stronger the absorbance is. Thus, it could be believed that radiation of PL in the range 350–600 nm is re-absorbed by Ni–P nanorods more or less. In present experiments, the sample with large nanorod aspect ratio  $L/d$  possesses large volume ratio of Ni–P nanorods. As the volume ratio of Ni–P increases, the re-absorption of Ni–P increases and the PL intensity decreases. This kind of dependence of the PL intensity upon the volume ratio was also mentioned before [40]. Therefore, for the Ni–P/AAO nano-array composite structure, the decrease of the intensity of PL emission peak with increase of the nanorod aspect ratio can be explained by re-absorption by the Ni–P nanorods.

## Conclusions

Using ac electrodeposition, Ni–P nanorod arrays can be embedded into the pores of AAO membrane to form Ni–P/AAO nano-array composite structures. By adjusting the deposition time, the composite structures with a certain aspect ratio of Ni–P nanorods can be synthesized. Present experiments show that with the increase of the nanorod aspect ratio, the optical absorbance decreases in the ultraviolet region and increases in the visible region. In addition, the photoluminescence of the Ni–P/AAO nano-array composite structures decreases as the aspect ratio increases. The influence of the nanorod aspect ratio on the optical properties of the Ni–P/AAO nano-array composite structure is in qualitative accord with the prediction of the MG effective medium theory in the visible region and the simulation obtained using the Mie scattering theory in the ultraviolet region.

**Acknowledgements** This work was supported by FANEDD of China No. 200525, Natural Science Foundation of Hubei Province No.2005ABA027 and Science & Technology Program of Wuhan City No.200970634268.

## References

- Martin CR (1994) Science 266:1961
- Xia Y, Yang P, Sun Y, Wu Y, Mayers B, Gates B, Yin Y, Kim F, Yan H (2003) Adv Mater 15:353
- Cornelius TW, Brötz J, Chtanko N, Dobrev D, Miehe G, Neumann R, Toimil-Molares ME (2005) Nanotechnology 16: S246
- Liu J, Duan JL, Toimil-Molares ME, Karim S, Cornelius TW, Dobrev D, Yao HJ, Neumann R (2006) Nanotechnology 17:1922
- Karim S, Toimil-Molares ME, Balogh AG, Ensinger W, Cornelius TW, Khan EU, Neumann R (2006) Nanotechnology 17:5954

6. Whitney TM, Jiang JS, Searson PC, Chien CL (1993) *Science* 261:1316
7. Yi G, Schwarzacher W (1999) *Appl Phys Lett* 74:1746
8. Molares EMT, Buschmann V, Dobrev D, Neumann R, Scholz R, Schuchert IU, Vetter J (2001) *Adv Mater* 13:62
9. Xu DS, Xu YJ, Chen DP, Guo GL, Gui LL, Tang YQ (2000) *Adv Mater* 12:520
10. Sapp SA, Lakshmi BB, Martin CR (1999) *Adv Mater* 11:402
11. Preston CK, Moskovits M (1993) *J Phys Chem* 97:8495
12. Foss CA Jr, Hornyak GL, Stockert JA, Martin CR (1994) *J Phys Chem* 98:2963
13. Foss CA Jr, Hornyak GL, Stockert JA, Martin CR (1993) In: *Proceedings of materials research society symposium on nanomaterials*, vol 286. Boston, MA, p 431
14. Hornyak GL, Patrissi CJ, Martin CR (1997) *J Phys Chem B* 101:1548
15. Al-Rawashdeh N, Foss CA Jr (1997) *Nanostruct Mater* 9:383
16. Brenner A, Riddell GE (1946) *J Res Natl Bur Stand* 37:31
17. Chiriac H, Moga AE, Urse M, Paduraru I, Lupu N (2004) *J Magn Magn Mater* 272–276:1678
18. Feldheim DL, Foss CA Jr (2002) *Metal nanoparticles: synthesis, characterization and application*. Marcel Dekker, New York
19. Wang QQ, Han JB, Guo DL, Xiao S, Han YB, Gong HM, Zou XW (2007) *Nano Lett* 7:723
20. Zong RL, Zhou J, Li Q, Du B, Li Q, Fu M, Qi XW, Li LT (2004) *J Phys Chem B* 108:16713
21. Chen HM, Hsin CF, Liu RS, Hu SF, Huang CY (2007) *J Electrochem Soc* 154:k11
22. Guo DL, Fan LX, Sang JP, Liu YF, Huang SY, Zou XW (2007) *Nanotechnology* 18:405304 (4 pp)
23. Masuda H, Fukuda F (1995) *Science* 268:1466
24. Yin AJ, Li J, Jian W, Bennett AJ, Xu JM (2001) *Appl Phys Lett* 79:1039
25. Duan JL, Liu J, Yao HJ, Mo D, Hou MD, Sun YM, Chen YF, Zhang L (2008) *Mater Sci Eng B* 147:57
26. Zong RL, Zhou J, Li B, Fu M, Shi SK, Li LT (2005) *J Chem Phys* 123:094710-1–094710-5
27. Tang HJ, Wu FQ, Zhang S (2006) *Appl Phys A* 85:29
28. Gao TR, Chen ZY, Peng Y, Li FS (2002) *Chin Phys* 11:1307
29. Locharoenrat K, Sano H, Mizutani G (2007) *Sci Technol Adv Mater* 8:277
30. Halperin WP (1986) *Rev Mod Phys* 58:533
31. Aspnes DE (1982) *Thin Solid Films* 89:249
32. Van de Hulst HC (1981) *Light scattering by small particles*. Dover, New York
33. Foss CA Jr, Tierney MJ, Martin CR (1992) *J Phys Chem* 96:9001
34. Al-Rawashdeh NAF, Sandrock ML, Seugling CJ, Foss CA Jr (1998) *J Phys Chem B* 102:361
35. Bohren CF, Huffman DR (1983) *Absorption and scattering of light by small particles*. Wiley, New York
36. Barber PW, Hill SC (1990) *Light scattering by particles: computational methods*. World Scientific, River Edge, NJ
37. Asano S (1979) *Appl Opt* 18:712
38. Asano S, Yamamoto G (1975) *Appl Opt* 14:29
39. Varadan VK, Varadan VV (1980) *Acoustic, electromagnetic and elastic wave scattering: focus on the T-matrix approach*. Pergamon, New York
40. Guo DL, Fan LX, Wang FH, Huang SY, Zou XW (2008) *J Phys Chem C* 112:17952